

NUMERICAL INVESTIGATION ON THE CRITICAL TRANSITION CAPILLARY NUMBER BETWEEN BYPASS AND RECIRCULATING FLOW REGIMES ON THE DISPLACEMENT OF A LIQUID IN CAPILLARY TUBES

Raphael David Aquino Bacchi,

Group of Flow of Complex Fluids, Applied Mechanic Laboratory, PGMEC, Department of Mechanical Engineering, Federal University Fluminense, Passo da Pátria Street 156, Niterói, 24210-240, RJ, Brazil

Roney Leon Thompson, roney@cv.uff.br

Group of Flow of Complex Fluids, Applied Mechanic Laboratory, PGMEC, Department of Mechanical Engineering, Federal University Fluminense, Passo da Pátria Street 156, Niterói, 24210-240, RJ, Brazil

Edson José Soares, edson@ct.ufes.br

Group of Flow of Complex Fluids, Department of Mechanical Engineering, Federal University of Espírito Santo, Fernando Ferrari Avenue, 514, Goiabeiras, 29060-900, Vitória, ES, Brazil.

Abstract. An elliptic mesh generation technique, with the Galerkin Finite Element Method is used to compute the interface of the two-phase flow problem of the displacement of a liquid. In the present work, besides fraction of mass deposit on the wall, special attention is given to the transition between two well-defined flow regimes: bypass flow and fully-recirculating flow. Comparison with the classical flow patterns predicted by Taylor (1961) for gas displacing a Newtonian liquid is made by two branches of analysis: the liquid-liquid displacement as a function of viscosity ratio and a gas displacing a non-Newtonian fluid. The non-Newtonian constitutive equations employed are: a power-law (shear-thinning and shear-thickening cases) and the Papanastasiou-Bingham model. For the liquid-liquid displacement it is found that a decrease in the viscosity ratio between displaced and displacing fluids increases the critical capillary number, Ca_c in which transition occurs. For the power-law case, depending on the behavior index, n , Ca_c has opposite tendencies: it decreases for shear-thinning liquids and increases for shear-thickening ones. The viscoplastic case analyzed shows a tendency similar to the shear-thinning liquid. In the viscoplastic and pseudoplastic case it was found an interesting type of intermediate flow regime which is not present in the Newtonian transition.

Keywords: displacement of a liquid, non-Newtonian Fluids, bypass flow, finite element method, interfacial tension.

1. INTRODUCTION

The displacement of a fluid by gas injection is a phenomenon that occurs in many industrial processes. Figure (1) shows the flow of a gas displacing a fluid in a capillary tube. The tube is initially occupied by the liquid when a gas is injected. When inertia effects can be neglected, the interfacial front reaches a constant velocity even for a constant pressure process, as reported in Taylor (1961) and Cox (1962). In this case, the dimensionless parameter that governs the problem is the capillary number (Ca). This parameter signifies the ratio of the viscous to interfacial tension forces. For a constant flow rate process or negligible inertia, the usual expression for the capillary number is $Ca = \mu U / \sigma$ where, μ is the fluid viscosity, σ is the interfacial tension and U is the displacement velocity.

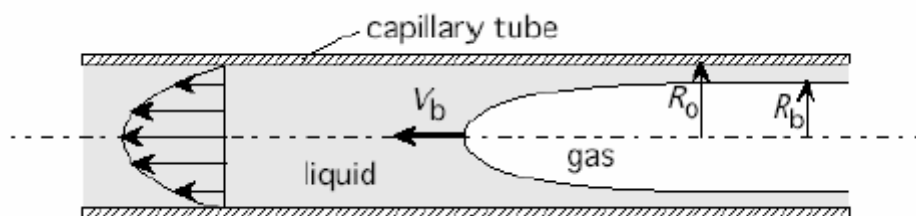


Figure 1 – Schematics of the problem.

Taylor (1961) studied this problem, for a quite large range of capillary number. In his theoretical analysis, he suggested three possible flow regimes of the liquid flow near the interface. The first one, a bypass flow, which would occur at high capillary numbers, the flow would pass completely and no recirculation would appear near the free surface. The other two have recirculation flow patterns. The second one, at a moderate capillary number, the liquid would have a timid recirculation and a stagnation point would arise in the liquid, after the tip of the interface. At low capillary numbers, a third streamline pattern would form when the recirculation of the liquid would have a surface

contact with the gas and in this case a stagnation ring would also be formed. Cox (1964) investigated experimentally the streamline patterns suggested by Taylor and found the two extreme cases suggested, namely, a bypass flow and a fully-recirculating flow for high and low capillary numbers, respectively.

The main objective of this work is to investigate numerically how the flow regimes suggested by Taylor (1961), in his classical work concerning gas-liquid displacement of a Newtonian fluid, are affected by changes on the rheology of the fluids involved. The non-Newtonian constitutive equations employed are: a power-law (shear-thinning and shear-thickening cases) and the Papanastasiou-Bingham model.

2. PHYSICAL FORMULATION

2.1. Conservation equations and boundary conditions

The physical model to describe the displacement of a fluid of viscosity η by a long gas bubble is now presented.

The displacing bubble is translating steadily with speed U . To simplify the analysis, the governing equations are written with respect to a moving reference frame located at the tip of the interface. In this frame of reference, the flow is steady and the wall is moving with velocity U . The geometry analyzed is an axisymmetric tube of radius R . The liquid is assumed to be incompressible, and the flow is laminar and the inertia is negligible. The velocity and pressure fields are governed by the continuity and momentum equations. In cylindrical coordinates, these governing equations are written as.

$$\frac{1}{r} \frac{\partial}{\partial r} (rv) + \frac{\partial u}{\partial x} = 0 \quad (1)$$

$$\rho \left(v \frac{\partial v}{\partial r} + u \frac{\partial v}{\partial x} \right) = \frac{1}{r} \frac{\partial}{\partial r} (rT_{rr}) - \frac{T_{\theta\theta}}{r} + \frac{\partial T_{rx}}{\partial x} \quad (2)$$

$$\rho \left(v \frac{\partial u}{\partial r} + u \frac{\partial u}{\partial x} \right) = \frac{1}{r} \frac{\partial}{\partial r} (rT_{rx}) + \frac{\partial T_{xx}}{\partial x} \quad (3)$$

Where u and v are respectively the axial and radial components of the velocity field \mathbf{u} and the quantities $\tau_{xx}, \tau_{rx}, \tau_{rr}$, and $\tau_{\theta\theta}$ are the components of the stress tensor $\boldsymbol{\tau}$.

In order to facilitate the following description of the boundary conditions, the boundaries are labeled from 1 to 5, as illustrated in Fig. (2).

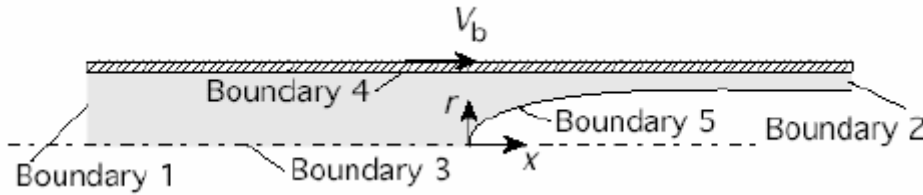


Figure 2. Flow domain for gas-displacement of liquid in a tube.

1) Far enough upstream of the interface, Boundary 4, the flow is taken to be fully developed and the pressure is assumed to be uniform:

$$\mathbf{n} \cdot \nabla \mathbf{u} = 0 \quad \text{and} \quad p = P_{in} \quad (4)$$

where \mathbf{n} is the unit vector normal to the boundary surface and p_{in} the pressure field.

2) Far enough downstream, Boundary 1, the flow is also assumed to be fully developed, but the pressure is not imposed:

$$\mathbf{n} \cdot \nabla \mathbf{u} = 0 \quad (5)$$

3) Along the symmetry axis, Boundary 2, both the shear stress and the radial velocity vanish:

$$(\mathbf{n} \cdot \mathbf{T}) \cdot \mathbf{t} = 0 \quad \text{and} \quad \mathbf{n} \cdot \mathbf{u} = 0 \quad (6)$$

where \mathbf{t} is a unit vector tangent to the boundary surface.

4) The no-slip and impermeability conditions are imposed along the tube wall, Boundary 3:

$$\mathbf{u} = U\mathbf{e}_x \quad (7)$$

where \mathbf{e}_x is the unit vector in the x-direction.

5) At the liquid-liquid interface, Boundary 5, the traction balances the capillary pressure, and there is no mass flow across the interface:

$$\mathbf{n} \cdot \mathbf{T} = \left(\frac{\sigma}{R_m} - P_0 \right) \mathbf{n} \quad (8)$$

$$\mathbf{n} \cdot \mathbf{u} = 0 \quad (9)$$

In Eq. (10), $1/R_m$ is the local mean curvature of the interface, defined as

$$\frac{1}{R_m} \mathbf{n} = \frac{1}{\sqrt{x_s^2 + r_s^2}} \frac{\partial \mathbf{t}}{\partial s} - \frac{x_s}{r\sqrt{x_s^2 + r_s^2}} \mathbf{n} \quad (10)$$

where \mathbf{t} is the unit tangent vector to the free surface, s is the arc-length curvilinear coordinate along the interface in the r - x plane and $x_s = \partial x / \partial s$ and $r_s = \partial r / \partial s$ are spatial derivatives with respect to s .

2.2. Constitutive equations

In order to close the set of differential equations, the stress tensor was related with the kinematics of the flow by the Generalized Newtonian Fluid model. In this model, the stress tensor is given by

$$\mathbf{T} = -p\mathbf{I} + \eta(\dot{\gamma})\dot{\gamma} \quad (11)$$

where $\dot{\gamma} = \nabla \mathbf{u} + \nabla \mathbf{u}^T$ is the rate of strain tensor. The scalar quantity $\eta(\dot{\gamma})$ is the viscosity function, and $\dot{\gamma} \equiv \sqrt{\frac{1}{2} \text{tr}(\dot{\gamma} \cdot \dot{\gamma})}$ is the deformation rate. The viscosity function $\eta(\dot{\gamma})$ depends on the specific class of material employed. In the present work we have three cases

2.2.1 Newtonian material

$$\eta = \mu$$

where $\eta = \mu$ is a constant.

2.2.1 Power law material

$$\eta = \kappa \dot{\gamma}^{n-1} \quad (12)$$

where κ is the consistency and n is the behavior index of the fluid.

2.2.2 Viscoplastic Papanastasiou's material

where τ_0 is the yield stress, μ is an asymptotic viscosity value at high shear rate and c is a regularization parameter. A viscoplastic material is generally described as a material which flows only when the stress is above a particular level, the material yield stress. The Bingham model which was the first model proposed to capture such behavior has the inconvenient feature of being discontinuous and, therefore, it leads to numerical difficulties. Papanastasiou (1987) suggested the use of a regularization parameter in order to have a smooth transition between non-yielded and yielded

state. As suggested by a number of works presented on literature (e.g. Dimakopoulos and Tsamopoulos (2003)), $1000 c C \dot{\gamma}_c = 1000$. For this value of the constant c , the Papanastasiou's viscosity function tends to the perfect plastic model, given by the Bingham viscosity function.

$$\eta = \mu + \frac{\tau_0(1 - e^{-c\dot{\gamma}})}{\dot{\gamma}} \quad (13)$$

3. SOLUTION METHOD

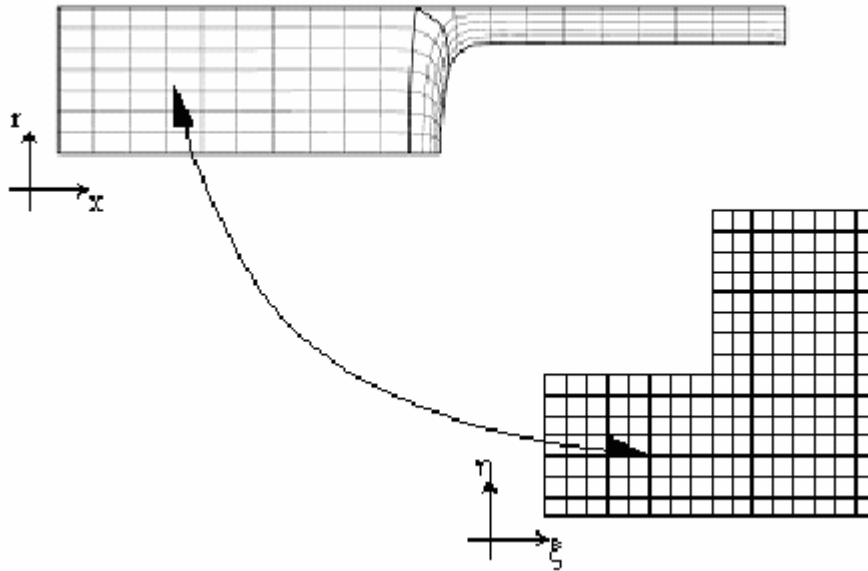
Since the flow domain is unknown a priori, the set of differential equations and boundary conditions written for the physical domain has to be transformed to an equivalent set, defined in a known reference domain. This transformation is made by a mapping $\mathbf{x} = \mathbf{x}(\xi)$ that connects the two domains, as shown in Fig. (3). The inverse of the mapping, the so-called mesh generation equations, is governed by a pair of elliptic differential equations with variable diffusion coefficients. The coordinates ξ and η of the reference domain satisfy

$$\nabla \cdot (D_\xi \nabla \xi) = 0 \text{ and } \nabla \cdot (D_\eta \nabla \eta) = 0 \quad (14)$$

Where D_η and D_ξ are diffusion-like coefficients used to control gradients in coordinate potentials. This subject is better discussed on papers of Kistler and Scriven (1983) and Santos (1991).

Along the solid walls and synthetic inlet and outlet planes, the boundary is located by imposing a relation between coordinates x and y , and stretching functions are used to distribute the nodal points of the finite element mesh along the boundaries. The fluid-fluid interface is located by imposing the kinematic condition, Eq. (9).

PHYSICAL DOMAIN



REFERENCE DOMAIN

Figure 3 – Mapping between the physical and reference domains. Gas-liquid displacement.

The differential equations that govern the problem and the mapping (mesh generation) equations were solved all together by the Galerkin/Finite Element Method. Biquadratic basis functions (ϕ_j) were used to represent the velocity and nodal coordinates, while linear discontinuous functions (χ_j) were employed to expand the pressure field. The velocity, pressure and node position are represented in terms of appropriate basis functions.

$$u = \sum U_j \phi_j; v = \sum V_j \phi_j; p = \sum P_j \chi_j; x = \sum X_j \phi_j; r = \sum R_j \phi_j \quad (15)$$

The coefficients of the expansions are the unknown of the problem:

$$C = [U_j \ V_j \ P_j \ X_j \ R_j]^T \quad (16)$$

The corresponding weighted residuals of the Galerkin method related to conservation of momentum, mass and mesh generation are:

$$R^i_{mx} = \int_{\bar{\Omega}} \left\{ \rho \phi_i \left(u \frac{\partial u}{\partial x} + v \frac{\partial u}{\partial r} \right) + \frac{\partial \phi_i}{\partial x} T_{xx} + \frac{\partial \phi_i}{\partial r} T_{xr} \right\} r \|\mathbf{J}\| d\bar{\Omega} - \int_{\bar{\Gamma}} \mathbf{e}_x \cdot (\mathbf{n} \cdot \mathbf{T}) \phi_i r \frac{d\Gamma}{d\bar{\Gamma}} d\bar{\Gamma} \quad (17)$$

$$R^i_{mr} = \int_{\bar{\Omega}} \left\{ \rho \phi_i \left(u \frac{\partial v}{\partial x} + v \frac{\partial v}{\partial r} \right) + \frac{\partial \phi_i}{\partial x} T_{xr} + \frac{\partial \phi_i}{\partial r} T_{rr} + \frac{\phi_i}{r} T_{\theta\theta} \right\} r \|\mathbf{J}\| d\bar{\Omega} - \int_{\bar{\Gamma}} \mathbf{e}_r \cdot (\mathbf{n} \cdot \mathbf{T}) \phi_i r \frac{d\Gamma}{d\bar{\Gamma}} d\bar{\Gamma} \quad (18)$$

$$R^i_{mx} = \int_{\bar{\Omega}} \rho \chi_i \left(\frac{\partial u}{\partial x} + \frac{1}{r} \frac{\partial}{\partial r} (rv) \right) r \|\mathbf{J}\| d\bar{\Omega} \quad (19)$$

$$R^i_x = - \int_{\bar{\Omega}} [D_\xi \nabla \xi \cdot \nabla \phi_i] \|\mathbf{J}\| d\bar{\Omega} + \int_{\bar{\Gamma}} D_\xi (\mathbf{n} \cdot \nabla \xi) \phi_i \frac{d\Gamma}{d\bar{\Gamma}} d\bar{\Gamma} \quad (20)$$

$$R^i_r = - \int_{\bar{\Omega}} [D_\eta \nabla \eta \cdot \nabla \phi_i] \|\mathbf{J}\| d\bar{\Omega} + \int_{\bar{\Gamma}} D_\eta (\mathbf{n} \cdot \nabla \eta) \phi_i \frac{d\Gamma}{d\bar{\Gamma}} d\bar{\Gamma} \quad (21)$$

As indicated above, the system of partial differential equations and boundary conditions is reduced to a set of simultaneous algebraic equations for the coefficients of the basis functions of all the fields. This set is non-linear and sparse. It was solved by Newton's method. In order to improve the initial guess there were necessary to solve intermediate problems. The first successful free surface flow was computed using a fixed boundary flow field with slippery surface in place of the free boundary as the initial condition for Newton's method. The linear system of equations at each Newton iteration was solved using a frontal solver. A mesh convergence analysis was done increasing the elements number until the solution changed by less that 1% between successive refinements. Representative mesh is shown in Fig (4).

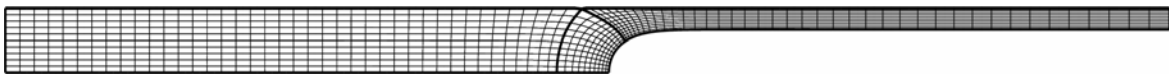


Figure 4. Representative finite element mesh for the gas-liquid displacement with 900 elements and 17904 unknowns.

4. THEORETICAL ANALYSIS

4.1 Fraction of liquid

The amount of the liquid 2 that remains on the capillary wall is usually reported in terms of the mass fraction of liquid that is not displaced m , or simply by the liquid film thickness left on the wall. The two forms are related by

$$\begin{aligned}
m &= \frac{\text{mass left on wall}}{\text{total mass}} = 1 - \frac{\text{displaced mass}}{\text{total mass}} \\
&= 1 - \left(\frac{D_b}{D_0} \right)^2 = 1 - \left(1 - \frac{2h_\infty}{D_0} \right)^2
\end{aligned} \tag{24}$$

The mass fraction of the liquid left on the tube wall can be evaluated using the mass conservation principle for the liquid in a control volume containing the tip of the interface and attached to it. For a gas displacement of a noninertial incompressible Newtonian liquid, the dimensionless parameter that governs the problem is the Capillary number. Since this number is based on the viscosity of the liquid, for a non-Newtonian fluid, in which viscosity is not constant for an isothermal flow, it is necessary to choose a characteristic viscosity of the problem. For this purpose the viscosity function is evaluated at the characteristic deformation rate of the flow which in this problem is $\dot{\gamma} = V_b / R_0$. Besides that, for each class of material studied there is a second dimensionless parameter which is associated to a rheological property.

4.2 Power-law fluid

The Capillary number for the power-law fluid is given by

$$Ca = \frac{\eta_c V_b}{\sigma} = K \left(\frac{V_b}{R_0} \right)^{n-1} \frac{V_b}{\sigma} = \frac{K}{\sigma} \frac{(V_b)^n}{R_0^{n-1}}$$

The rheological dimensionless parameter is the power-law index n .

4.3 Viscoplastic Papanastasiou's material

$$Ca = \frac{\eta_c V_b}{\sigma} = \frac{(\mu + \tau_0 / \dot{\gamma}_c) V_b}{\sigma} = \frac{[\mu + (\tau_0 R) / V_b] V_b}{\sigma}$$

And the second parameter is the dimensionless yield stress which is

$$\tau'_0 = \frac{\tau_0}{\mu (V_b / R) + \tau_0}$$

5. RESULTS

Figure (5) shows the effect of behavior index, n , on the fraction of mass, m , deposited on the tube wall as a function of capillary number (in a logarithm scale) for the gas-liquid. For the entire range of analysis it can be seen that m increases as behavior index is incremented.

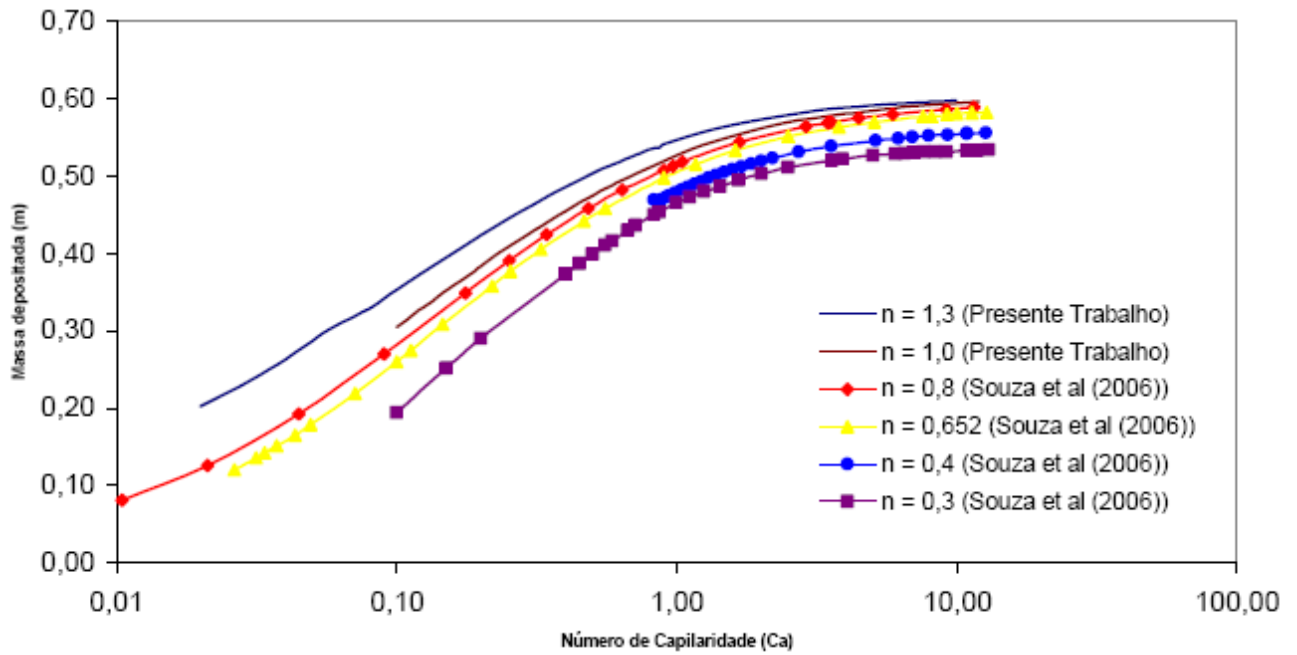
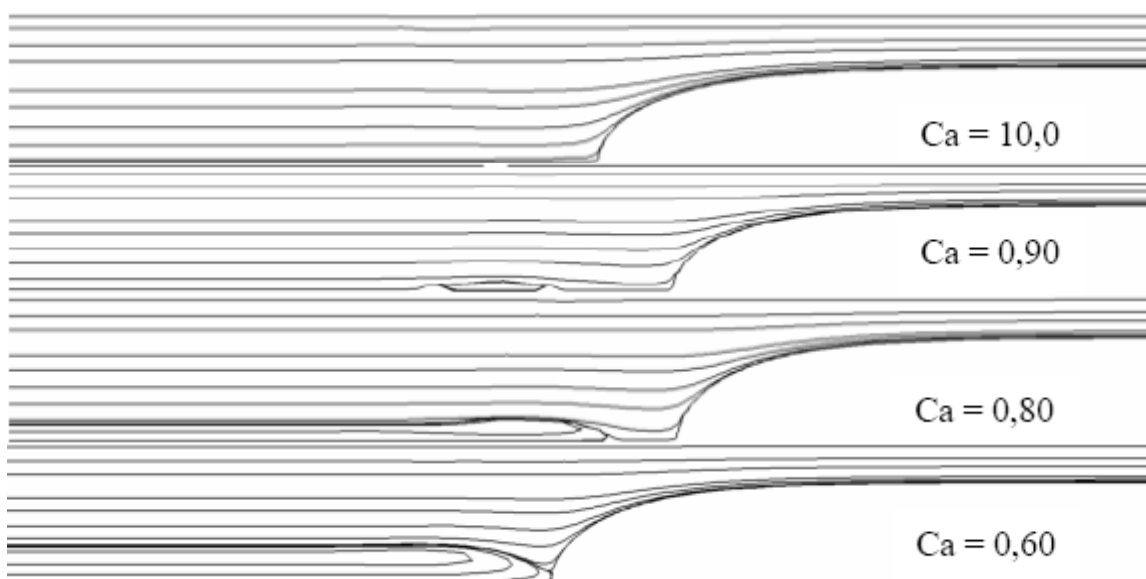


Figure 5 – Fraction of mass deposited on the tube wall as a function of the behavior index. Comparison with the work done by Sousa et al. (2007)

Figures (6), (7), (8), and, (9) show flow patterns for the gas displacement of a non-Newtonian fluid. Figures (6), and (7) explore power-law transition between bypass and fully-recirculating flow regimes for a shear-thickening ($n=1.3$) and a shear-thinning ($n=0.652$) fluid respectively. As we can see, the critical capillary transition has opposite tendencies if we take the Newtonian result. While in the shear-thickening fluid the critical capillary number increases its value, in the shear-thinning fluid the critical capillary number decreases. It is worth noting that on the two cases, the flow regimes of transition are intrinsically different from the Newtonian case. In the Newtonian case the recirculation of the displaced liquid first appears from the left boundary, in the case where we are decreasing the Capillary number. In contrast, in the shear-thickening case the recirculation appears in the middle of the liquid and migrates toward the left boundary and in the shear-thinning case the recirculation appears at the tip of the bubble and migrates toward the left boundary.



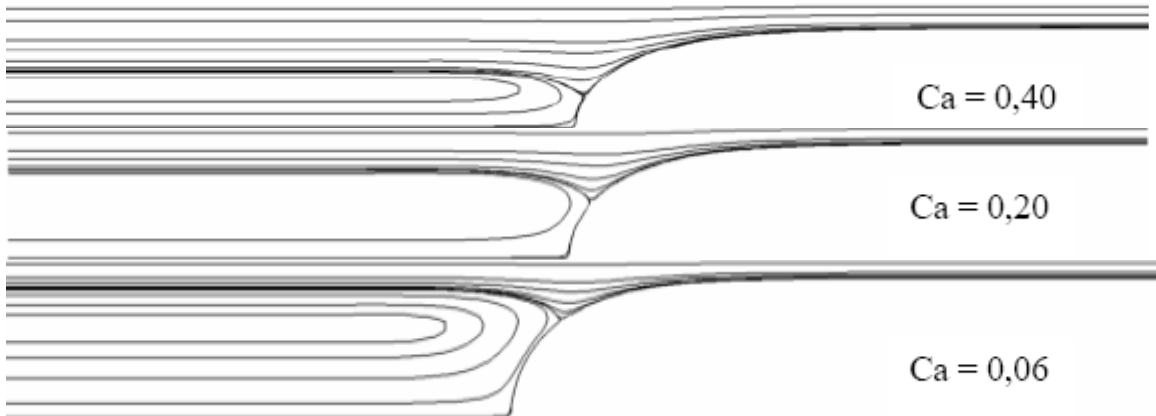


Figure 6– Streamline patterns near the tip of the interface: gas displacing a shear-thickening power-law fluid with behavior index $n=1.3$. From bypass to fully-recirculation flow regime.

The viscoplastic case shown in Figs.(8), and (9), shows a similar behavior to the one presented by the shear-thinning case, i.e. the critical Capillary number is lower and the recirculation appears near the tip of the bubble.

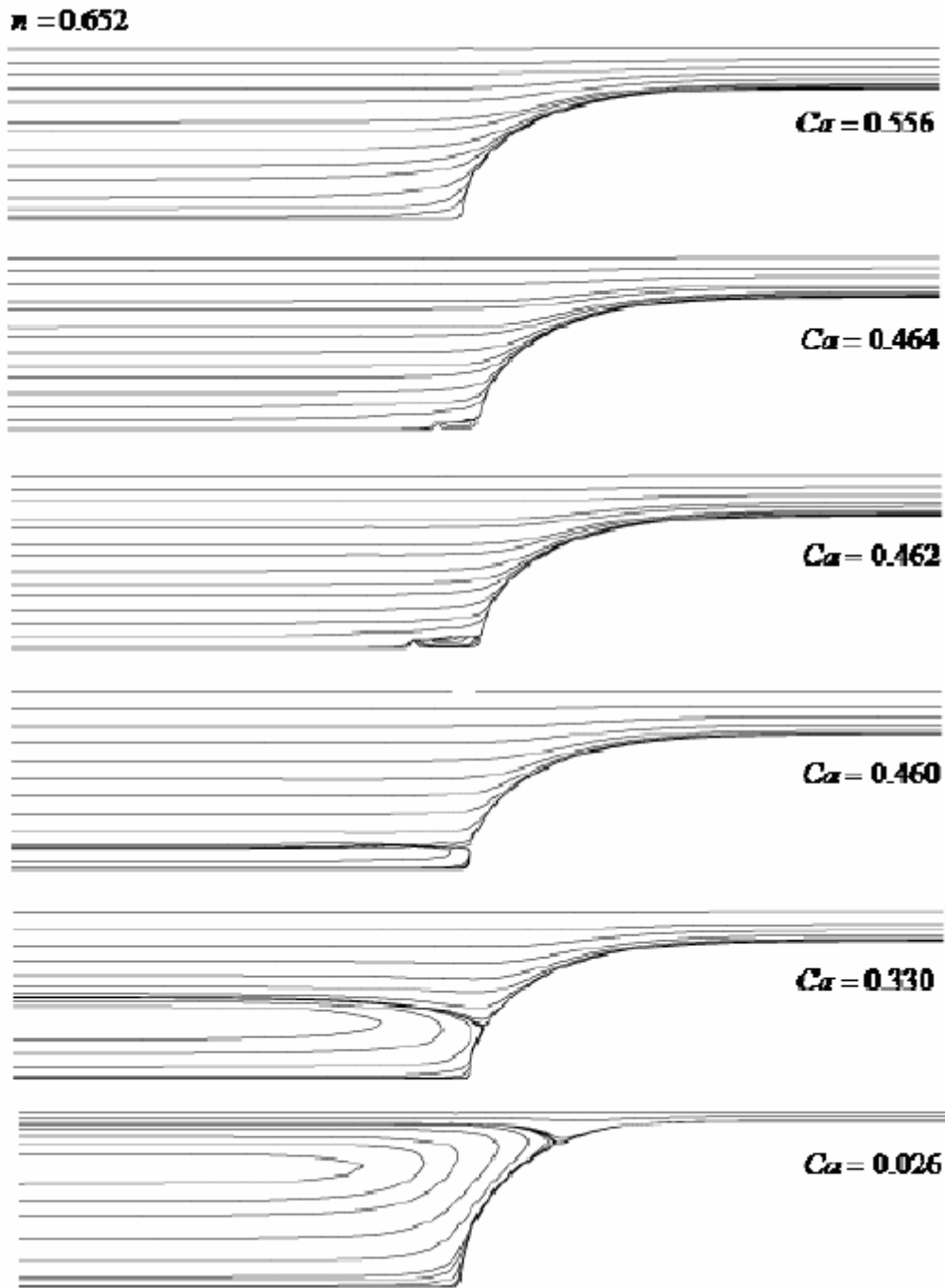


Figure 7 – Streamline patterns near the tip of the interface: gas displacing a shear-thinning power-law fluid with behavior index $n=0.652$. From bypass to fully-recirculating flow regime.

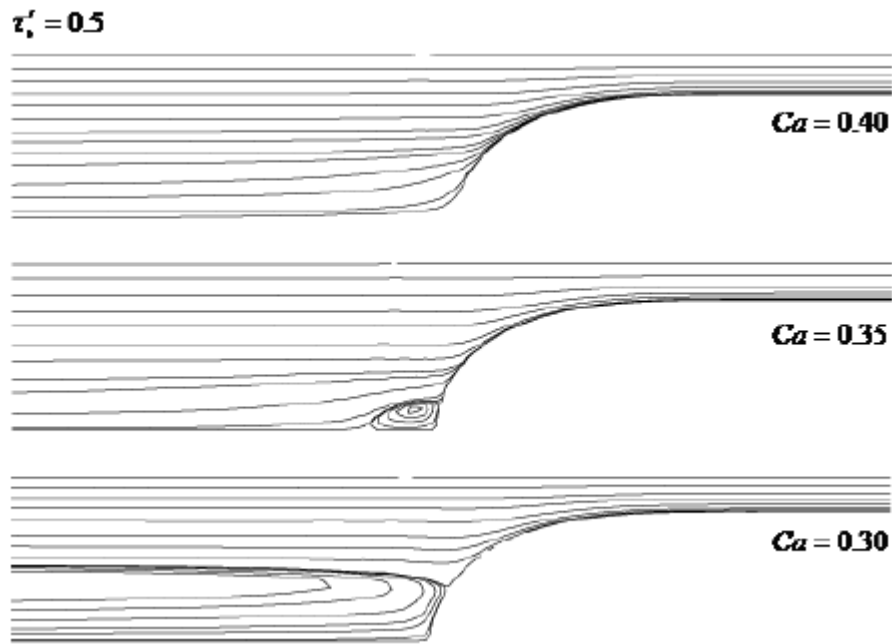


Figure 8 – Streamline patterns near the tip of the interface: gas displacing a viscoplastic Papanastasiu’s material with dimensionless yield stress $\tau_0' = 0.5$. From bypass to fully-recirculating flow regime.

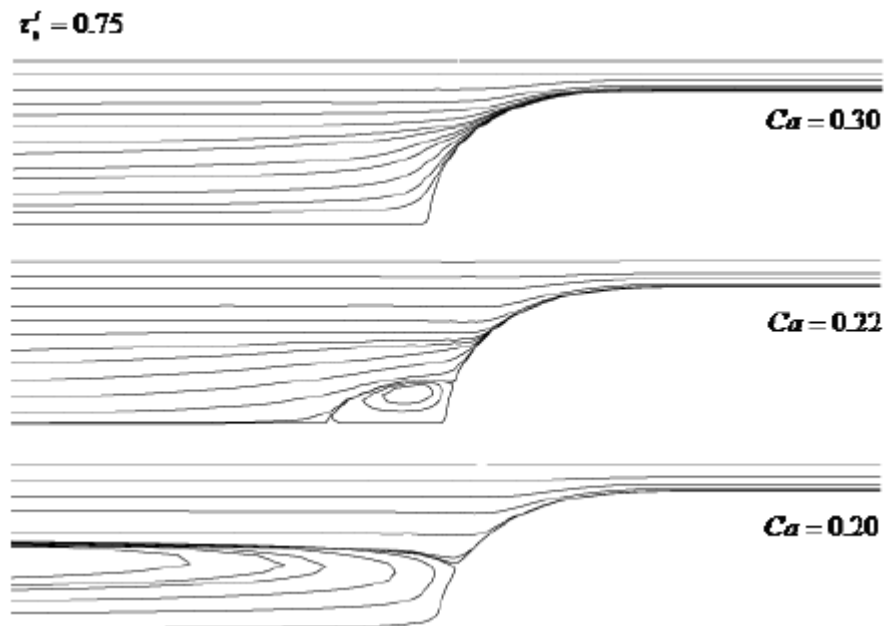


Figure 9– Streamline patterns near the tip of the interface: gas displacing a viscoplastic Papanastasiu’s material with dimensionless yield stress $\tau_0' = 0.75$. From bypass to fully-recirculating flow regime.

5. CONCLUSIONS

An axisymmetric model of the flow near the upstream fluid-fluid interface of a long bubble penetrating through a liquid in a capillary tube was presented. The presence of the interface makes the problem complex, since the domain in which the differential equations are integrated is unknown a priori. A fully coupled formulation was used and the differential equations were solved via the Galerkin finite element method. The main contribution of the present work was to investigate the influence of the transition between two well defined flow regimes: bypass flow and fully-recirculating flow. Comparison with the classical flow patterns predicted by Taylor (1961) for gas displacing a Newtonian liquid is

made by a gas displacing a non-Newtonian fluid. The non-Newtonian constitutive equations employed are: a power-law (shear-thinning and shear-thickening cases) and the Papanastasiou-Bingham model. For the power-law case, depending on the behavior index, n , Ca has opposite tendencies: it decreases for shear-thinning liquids and increases for shear-thickening ones. The viscoplastic case analyzed shows a tendency similar to the shear-thinning liquid. In the viscoplastic and power-law cases it was found an interesting type of intermediate flow regime which is not present in the Newtonian transition.

6. ACKNOWLEDGEMENTS

The authors are thankful to CAPES, MCT/CNPq and ANP, for their financial support.

7. REFERENCES

- Cox, B. G., 1962, "On Driving a Viscous Fluid Out of a Tube," *Journal of Fluid Mechanics*, Vol. 14, pp. 81–96.
- Cox, B.G., 1964, "An experimental investigation of the streamlines in viscous fluid expelled from a tube", *Journal Fluid Mechanics*, Vol. 20 pp. 193–200.
- Dimakopoulos, y., Tsamopoulos, J., 2003, "Transient displacement of a viscoplastic material by air in straight and constricted tubes", *J. Non-Newton. Fluid Mech. Voll.* 112 pp. 43–75.
- Kistler, F., Scriven, L.E.S., 1983, "Coating flow theory by finite element and asymptotic analysis of the Navier–Stokes system", *Int. J. Numer. Meth. Fluids* Vol. 43 pp 207.
- Papanastasiou, T. C., 1987, "Flows of materials with yield-stress", *J. Rheol.* Vol. 31, pp. 385-404.
- Santos, J.M., "Two-phase cocurrent downflow through constricted passages", Ph.D. Thesis, University of Minnesota, MN, USA, 1991.
- Soares, E. J., Carvalho, M. S., Souza Mendes, P. R., 2005, "Immiscible liquid-liquid displacement in capillary tubes," *Journal of Fluids Engineering*, Vol. 127 (1), pp. 24-31.
- Taylor, G. I., 1961, "Deposition of a Viscous Fluid on the Wall of a Tube", *Journal of Fluid Mechanics*, Vol. 10, pp. 161–165.
- Sousa, D. A., Soares, E. J., Queiroz, R. S. and Thompson, R. L., 2007, "Numerical investigation on gas-displacement of a shear-thinning liquid and a viscoplastic material in capillary tubes", *J. non-Newtonian Fluid Mech.*, Vol. 144, pp. 149-159.

8. RESPONSIBILITY NOTICE

The authors are the only responsible for the printed material included in this paper.